Available online at www.sciencedirect.com
SCIENCE DIRECT
Catalysis Today 101 (2005) 93–107
CATALYSIS TODAY
www.elsevier.com/locate/cattod

Reduction of N_2O over carbon fibers promoted with transition metal oxides/hydroxides

Teresa Grzybek [a,*], Jerzy Klinik [a], Barbara Dutka [a], Helmut Papp [b], Vladimir Suprun [b]

[a] *Faculty of Fuels and Energy, University of Science and Technology, 30-059 Kraków, Poland*
[b] *Faculty of Chemistry and Mineralogy, University of Leipzig, 04103 Leipzig, Germany*

Abstract

Reductions of N_2O on oxides/hydroxides of nickel, cobalt or manganese supported on carbon fibers were studied. Supports and catalysts were characterized by low temperature argon sorption, temperature-programmed desorption (TPD) of surface oxides and temperature-programmed desorption of ammonia (TPAD), X-ray photoelectron spectroscopy (XPS) and temperature-programmed reduction (TPR). Conversion of N_2O depended on the initial pretreatment of the support, the origin of the effect lying in a different distribution of active material. The differences in distribution influenced also the mobility of surface oxygen. The presence of more labile oxygen resulted in its easier transfer and faster formation of CO_2.

Keywords: N_2O reduction; Carbon fibers; XPS; TPR

1. Introduction

Acid treatment of carbonaceous materials is known to change its surface chemistry. The presence of acidic groups on the surface of carbonaceous materials in turn influences the dispersion of active phase and catalytic activity, as well as selectivity in NO reduction with ammonia or carbons, and NH_3 oxidation to N_2 (and N_2O). NO reduction with carbon on active carbon-supported catalysts [1–8] and NO reduction with NH_3 on both active carbon- and carbon fiber-supported catalysts [9–17] have been studied extensively in recent years. Several interesting facts were observed:

i. There was an influence of the ash content and composition on catalytic reduction of NO with NH_3 [9]. Similar effects were observed for NO reduction with carbon [1].
ii. Acidic pretreatment of carbonaceous materials influenced their activity (cf. SCR activity for carbonaceous materials promoted with oxides/hydroxides of Mn [10–12]). The overall result of acidic pretreatment depended, however, on its conditions. Mainly, the type [11,18,19] and the temperature of acid [10,20] and the time of treatment [11] influenced the catalytic activity through the change in the type and the number of oxygen-containing surface groups. The formation of acidic species such as carboxylic and lactonic groups by the use of HNO_3 [18] or to a smaller extent by H_2SO_4 [11], increased the activity while the formation of more stable surface groups such as carbonyls or phenols by the use of HCl deactivated the catalysts [18].
iii. Selectivity to N_2 in the above-mentioned reactions and thus the presence or absence of N_2O in the products seems to be connected with the crystallite size of MeO_x, smaller crystallites of active material producing less N_2O. This was found for active carbon-supported MnO_x [10] or carbon fibers promoted with NiO [21]. The formation of N_2O is not quite understood. Curtin et al. [22] showed for copper oxide supported on Al_2O_3 that N_2 and N_2O are formed through dissociative chemisorption of NO thus leading to a pool of N species on the surface. They may be converted into N_2 or through the reaction of N with NO into N_2O. A decrease in the availability of surface lattice oxygen species in the

* Corresponding author. Tel.: +48 12 6172119; fax: +48 12 6172066.
E-mail address: grzybek@uci.agh.edu.pl (T. Grzybek).

0920-5861/$ – see front matter © 2005 Elsevier B.V. All rights reserved.
doi:10.1016/j.cattod.2005.01.006

reaction system, which may be reduced e.g. by the addition of SO_2 to the feed led to a lower formation of N_2O. Similar effects were found for active carbon-based catalysts or montmorillonites covered with carbon promoted with MnO_x [23].

On the other hand, it is believed that the mechanism of N_2O and NO reduction by carbon are essentially the same and can be summarized as [19]:

- dissociative adsorption of NO connected with N_2 formation either on a active catalyst site S and/or a free carbon site C_f

$$2S + 2NO \rightarrow 2S{-}O + N_2$$
$$2C_f + 2NO \rightarrow 2C{-}O + N_2$$

- oxygen transfer between the oxidized catalyst site S–O and carbon site C–O and surface carbon groups

$$C{-}O \rightarrow C(O)$$
$$S{-}O \rightarrow C(O)$$

- C_f site regeneration and catalytic site preparation

$$2C(O) \rightarrow CO_2 + C_f^*$$
$$2C_f^* + 2NO \rightarrow 2C{-}O + N_2 \rightarrow (CO_2 + C_f^*)$$

This model, however, does not take into account the possibility of higher or lower N_2O formation but only its decomposition. On the whole, it is not yet clear whether N_2O is formed in SCR as a primary product in a reaction parallel to the formation of N_2 and is then decomposed to N_2 on some catalysts in the mechanism suggested by the above-mentioned model or not formed due to lower oxygen availability as suggested by Curtin et al. [22]. Although extensive studies have been carried out on the heterogeneous catalytic decomposition of N_2O using oxide-supported catalysts, much less information is available on N_2O conversion over carbon-supported catalysts. Dandekar and Vannice [24] compared copper supported on active carbon, Al_2O_3, SiO_2 and ZSM-5 for N_2O decomposition. The efficient oxygen scavanging capability of carbon led to higher initial activities on Cu/C catalysts compared to Cu/ZSM-5 but the reaction was accompanied by a high gasification of carbon. The activity of Cu/C depended on the initial pretreatment of active carbon-initial oxidation with HNO_3 leading to an increase in activity in comparison to a heat pretreatment in H_2 at 1223 K, which resulted in no change in comparison to the untreated support. The pretreatment influenced additionally the stability of the catalysts. Labile surface oxygen and its mobility were found to play an important role in controlling the steady state behaviour of Cu. The mechanism was believed to involve dissociative adsorption of N_2O and the transfer of oxygen from active material to the carbon surface to form CO_2 or CO.

N_2O reduction was also studied by Zhu et al. on active carbon promoted with Ni [18] or Cu [19]. The role of oxidative pretreatment of the support was considered as (i) influencing the distribution of active material and, in consequence, providing better contact of catalytic material with carbon, making oxygen transfer easier and (ii) producing acidic groups which are useful for the release of carbon oxygen complexes.

There are, however, still some open questions e.g. how the process of N_2O decomposition on carbonaceous materials is influenced by (a) the amount of acidic groups introduced e.g. by HNO_3 at different temperatures or (b) the choice of metal oxide as active material.

In order to answer these questions, carbon fibers promoted with Ni, Co or Mn oxides/hydroxides were studied as catalysts for N_2O reduction. A detailed characterization of the supports and catalysts was carried out, and the article focuses additionally on how catalyst dispersion is affected by surface chemistry. In order to exclude the uncertain influence connected with the role of ash for the reduction of NO with NH_3 or with carbon, ashless carbonaceous materials, i.e. carbon fibers were used.

2. Experimental

2.1. Catalysts

A commercial carbon fiber Kynol (further designated as K) activated by the producer with water vapour was used as a support in the untreated or pretreated form. The pretreatment of carbon fiber K consisted of the oxidation with 40% aqueous solution of HNO_3 for 1 h either at 343 K or at boiling temperature. In the latter case, two versions of oxidation procedure were used: either in a closed or open system i.e. with or without the recirculation of the formed nitrogen oxides, respectively called methods I and II. The pretreatment parameters and designation of the supports are given in Table 1.

Active material oxides or hydroxides of Ni, Co or Mn (5 wt.% recalculated to the appropriate metal content) were introduced by wet impregnation onto oxidized (K-ox1 or K-ox3) or untreated (K) supports. K-ox2 was omitted, because as will be shown later in the text, the amount of acidic sites is the same for K-ox2 and K-ox3. The active material precursors were nitrates of Ni, Co or Mn.

The following experiments were carried out:

i. Determination of the texture, or in some cases, only the specific surface area by low temperature argon sorption at a relative pressure range p/p_0 of 0–1 or 0.05–0.35,

Table 1
The pretreatment parameters and designation of the studied carbon fibers

Sample	Pretreatment	Temperature	Method[a]
K	None	–	–
K-ox1	40% HNO_3	343 K	I
K-ox2	40% HNO_3	Boiling temperature	I
K-ox3	40% HNO_3	Boiling temperature	II

[a] Method I: in a closed system with a recirculation of the formed nitrogen oxides and method II: in an open system with the removal of the formed nitrogen oxides.

respectively, using a standard volumetric equipment. Before the adsorption experiment, the samples were outgassed at 393 K for several hours until the base pressure was lower than 10^{-5} mbar.

ii. The crystallographic state of active materials, especially the consequence of the possible participation of support in the reduction of active material was tested by X-ray diffraction (XRD) for K-Ni5 and K-Co5 calcined both at 523 and 673 K. The former temperature was selected because samples were calcined before reaction at 523 K while the latter coincides with temperature-programmed desorption of ammonia (TPAD) experiments and roughly with the last of experimental temperatures in N_2O reduction. No XRD was carried out for KMn5 because the reduction of MnO with carbon according to metallurgical data needs about 600 K higher temperatures than for the reduction of cobalt or nickel oxides and thus it is less reasonable to find metallic Mn in this case. Neither were the samples based on K-ox3 tested because XPS shows small crystallites and/or clusters of Mn, Ni or Co oxides present on this surface and thus XRD should show only amorphous system and additionally, as seen from our TPR spectra, the onset of reduction temperature for K-ox3-based samples shifts to higher temperatures in comparison to K-based one. Boot et al. [25] observed that cobalt oxide on Co/ZrO_2 was more difficult to reduce than in a physical mixture, which was attributed to the fact that cobalt oxide particles were in a dispersed state on the catalyst surface. Thus in our case, a similar effect may be responsible, if we take into account that worse-dispersed oxides (for K-Co5 and K-Ni5), which as discussed further in the text did not show any metallic Co or Ni, have a lower onset reduction temperature than K-ox3-Co5 (or K-ox3-Ni5, respectively). XRD experiments were carried out using Philips PV 3020 X'Pert diffractometer and Cu Kα line (λ = 0. 15418 nm).

iii. Temperature-programmed desorption (TPD) to determine surface oxides. A NETSCH STA409C apparatus equipped with a quadrupole mass spectrometer was used to determine the temperature-programmed desorption of H_2O, CO_2, O_2 and NO. The experiments were carried out on a 20 mg sample of the catalysts with 20 mg of Al_2O_3 as reference. At the beginning of each experiment, the sample was evacuated to 1 mbar in order to remove air and physically adsorbed gases. Then it was linearly heated at 10 K/min up to 1273 K in a stream of nitrogen. The weight loss and the intensities of mass numbers 18 (H_2O), 32 (O_2), 30 (NO) and 44 (CO_2) were recorded as a function of temperature.

iv. To determine the number and the strength of acid sites TPAD was performed under the following conditions: before reaction, samples were heated at 673 K in helium for 1 h (flow 25 ml/min). The temperature was chosen as it roughly corresponds with the highest studied N_2O reduction temperature, where extensive conversion was registered. Ammonia was adsorbed at 333 K and the system was flushed with helium for 1 h at the same temperature in order to remove physically adsorbed NH_3. The desorption followed with a heating rate of 10 K/min and the following mass numbers were registered: 18 (H_2O), 15 (NH_3), 28 (CO), 30 (NO) and 44 (CO_2, N_2O).

v. To determine the surface composition X-ray photoelectron spectroscopy (XPS) was measured. XPS was carried out on untreated samples i.e. without any preheating in order to get information concerning the way active material was introduced onto the surface; the lack of preheating is thus relevant because the supports were not calcined before impregnation. In order to test if extensive changes could occur during calcination, one sample (with the most uneven distribution K-Ni5) was calcined at 523 K (similarly as during the N_2O reduction experiment) and studied in XPS, as well. Additionally, the same sample was tested in XPS after the N_2O decomposition (in the absence of oxygen in reaction mixture). The spectra were recorded with a Leybold LH-10 spectrometer with a Mg Kα source and a multichannel plate analyzer, working in FAT mode (ΔE = constant) at a pass energy of 29.6 eV. For each sample, 10–50 scans were taken, depending on the intensity of a given peak. The samples were studied in the form of fibers packed onto the sample holder. The pressure in the main chamber during experiments was below 3×10^{-8} mbar. The spectra were smoothed and a non-linear background was subtracted. The spectra were fitted with a convolution of 50:50 Lorentzian and Gaussian curves. The main C 1s peak was used as an internal standard to calibrate binding energies (BE = 284.6 eV). The content of elements was calculated using the area of the main peaks (Mn 2p, Co and Ni $2p_{3/2}$, O 1s, C 1s and N 1s) and sensitivity factors of Wagner et al. [26].

vi. Temperature-programmed reduction was studied with an AMI-100 (Altamira Instruments) in 5% H_2/Ar (flow 25 ml/min) from 323 to 973 K with a heating rate of 10 K/min and was then held additionally at 973 K for 30 min. Before TPR, the samples were pretreated similarly as prior to the catalytic reaction by heating in helium (flow 25 ml/min) at 523 K for 2 h.

2.2. Catalytic experiments

Reduction of N_2O with carbon was carried out in a fixed bed microreactor under the following conditions: mass of catalyst: 200 mg; reaction mixture: 800 ppm N_2O in helium or 800 ppm N_2O and 3% O_2 in helium; flow: 100 ml/min; before reaction, the catalysts were calcined in order to decompose introduced nitrates to oxides/hydroxides in helium at 250 °C for 2 h (flow 100 ml/min). The amount of N_2O and CO_2 was registered by NDIR analyzer (Hartmann and Braun).

Table 2
Specific surface area S_{BET}, micropore and mesopore volume V_{mic} and V_{mes} and B constant from equation of Dubinin–Radushkevich for the studied supports

Sample	S_{BET} (m^2/g)	V_{mes} (cm^3/g)	S_{mes} (m^2/g)	V_{mic} (cm^3/g)	$B^a \times (10^7)$
K	783	0.011	8.48	0.300	3.30
K-ox 1	584	0.004	3.43	0.221	3.29
K-ox 2	598	0.009	7.41	0.241	4.90
K-ox 3	650	[a]	[a]	[a]	[a]

[a] Not measured.

3. Results and discussion

3.1. Characterization of the samples

3.1.1. Supports

3.1.1.1. Specific surface area and texture. Argon sorption isotherms are all of type I according to IUPAC classification, testifying a microporous character of the carbon fibers. The textural data for the supports are summarized in Table 2. From Table 2, it may be seen that:

i. the untreated and pretreated carbon fibers were microporous;
ii. oxidation led to the loss of S_{BET} from 783 to ca. 600 m^2/g and V_{mic} from 0.300 to ca. 0.23 ± 0.01 cm^3/g, irrespective of the oxidation temperature. However, there were differences in the micropore distribution depending on the temperature of pretreatment proven by the change in the B values of Dubinin–Radushkevich equation, which form a sequence $K \approx$ K-ox1 < K-ox2. The value of B is related to the porous texture of material; smaller values of B are connected with narrower micropores. Thus, the increase in B suggests the broadening of micropores through the formation of oxygen-contaning surface species and their subsequent gasification.

3.1.1.2. Temperature-programmed desorption (TPD) and temperature-programmed desorption of ammonia (TPA-D). Fig. 1 shows the results of TPD of surface oxides i.e. the amount desorbed for $m/e = 44$ (CO_2). Carbon dioxide corresponds to the acidic groups on the surface of carbonaceous materials (carboxylic groups or carboxylic anhydrides) [27]. The only other acidic groups present on the surface (of phenol type), which do not produce CO_2 are very weak and would not play a role in the deposition of active material, as previously reported for active carbons promoted with iron or manganese oxides or discussed fully for Cu/active carbons by Zhu et al. [18]. From Fig. 1, it is to be seen that oxidation at 343 K increases the number of carboxylic groups slightly. The effect of temperature is evident (the higher the temperature, the higher the amount of acidic sites). Oxidation at higher temperature results also in the formation of more stable (high temperature) acidic sites with a maximum at ca. 900 K, which do not exist for K-ox1 and K.

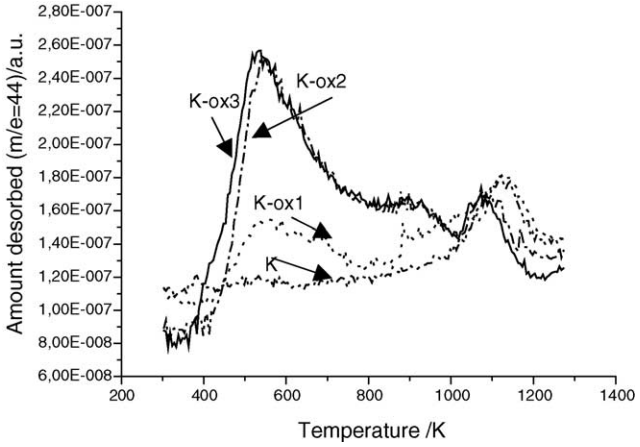

Fig. 1. The desorbed amount of $m/e = 44$ (CO_2) for carbon fibers untreated or oxidized under different conditions (TPD surface oxides).

Fig. 2 shows TPAD results for untreated or oxidized supports. One broad low temperature peak and an increase in amount desorbed of $m/e = 15$ (NH) starting from ca. 650 to 700 K, which is a part of an additional high temperature peak are observed. For some samples (catalysts K-Ni5, K-ox1-Ni5, K-Co5), the latter region contains additionally a well formed desorption maximum at ca. 850 K. There is not a clear explanation for the second peak, as carbonaceous materials do not contain highly acidic groups (and this would be suggested by high temperature TPAD). On the other hand, ammonia can react with carbonaceous materials at higher temperatures (e.g. 523 K [28] or 573 K [29]) leading to N-containing surface groups. The groups were different in form depending on the introduction stage; before carbonization and/or activation of carbon precursor or onto a previously carbonized and activated samples. Jurewicz et al. [29] found by XPS that in the latter case, nitrogen was present as mostly imine, imide, amide and amine groups, while in the former two cases, mostly pyridine and pyridone N was present. Therefore, it may be speculated that some

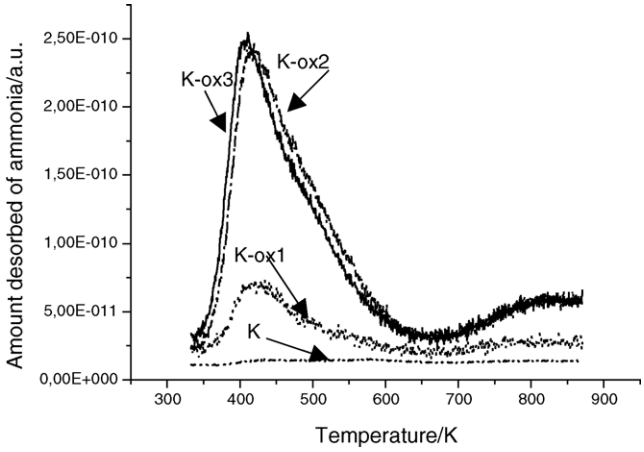

Fig. 2. The desorbed amount of $m/e = 15$ (NH_3) for carbon fibers untreated or oxidized under different conditions (TPAD).

chemisorbed ammonia survives during TPAD to temperatures high enough to react with carbonaceous material. The formed product decomposes then at higher temperatures. The argument is, however, speculative and most probably, as discussed above, has nothing to do with the acidity of to the studied samples and thus Table 5 (shown later, together with appropriate results for the catalysts) quotes only the areas of low temperature peaks. From Fig. 2 and Table 5, it may be seen that:

i. all carbon fibers both untreated and oxidized (K, K-ox1, K-ox2 and K-ox3) have one broad peak at low temperature although its asymmetry towards higher temperature suggests at least two types of acidic sites present with a broad distribution of desorption energy. The maximum temperature of desorption is at ca. 417 ± 5 K. The similarity of the shape of the peaks for all oxidized samples indicates that similar types of surface groups are formed;
ii. untreated support has a very small amount of acidic sites. The oxidation with 40% HNO_3 at 343 K (K-ox1) increased the amount of acidic groups 10 times in comparison to sample K. The use of a higher oxidation temperature, irrespective of the method used (I or II), resulted in the same amount of acidic sites; ca. four times higher than those formed during oxidation at lower temperature. Thus, the oxidation temperature has a primary influence on the formation of acidic groups on the surface of carbon fibers.

3.1.1.3. X-ray photoelectron spectroscopy (XPS). Table 3 presents the surface compositions of the studied supports. From Table 3, it may be seen that:

- the amount of carbon decreased and amount of surface oxygen increased upon oxidation;
- oxidation with nitric acid led to a small amount of N on the surface;
- O/C ratio increased in a sequence: K < K-ox1 < K-ox2 < K-ox3;
- O/C was very low for unoxidized carbon fibers.

A comparison of XPS with TPD ($m/e = 44$) and TPAD results reveals that there are differences in the total O/C ratios for K-ox2 and K-ox3, while no difference was detected by desorption methods, which show that the amount of acidic sites is similar for both samples. The smaller XPS O/C ratio for K-ox2 than for K-ox3 may be therefore connected with a smaller amount of non-acidic groups in this case, leading to desorption products different from CO_2. Zhu et al. [18] showed for active carbons promoted with Cu that non-acidic groups are, however, of small consequence for active material distribution in contrast to the presence of acidic groups, which lead to a more even distribution over the inner surface of the carbonaceous supports. From this point of view, supports K-ox2 and K-ox3 may be treated as very similar and thus only one of them (K-ox3) was further used as a support.

On the whole, the findings concerning role of HNO_3 and the influence of the conditions of its use on the formation of oxygen-containing surface species are in good agreement with the previous findings of the literature (e.g. [11,18,27,30–34]).

Table 3
Surface content of C, O and N (at.%) (C + N + O = 100 at.%) and atomic ratio O/C (at.%/at.%) for the studied supports

	C	O	N	O/C
K	91.7	8.3	–	0.091
K-ox1	84.9	14.6	0.6	0.172
K-ox2	82.2	17.8	traces	0.217
K-ox3	77.3	22.2	0.5	0.287

Table 4
Specific surface area, S_{BET}, for the studied catalysts

Sample	S_{BET} (m^2/g)
K-Ni5	287
K-ox1-Ni5	599
K-ox3-Ni1	545
K-ox3-Ni5	391
K-Co5	160
K-ox3-Co5	262
K-Mn5	279
K-ox3-Mn5	218

3.1.2. Catalysts

3.1.2.1. Specific surface area. Table 4 shows specific surface areas of the studied catalysts. Specific surface area depended on the pretreatment and the type of active material. The decrease in S_{BET} for K-ox3-based catalysts may be, in agreement with the discussion of XPS results, connected with small crystallites and/or clusters of active material deposited inside the porous system. In case of K-Ni5, K-Co5 and K-Mn5, the reason for the decrease may be the precipitation of bigger crystallites (as found by XPS) at the entrance to the pores.

Table 5
TPAD results: area of the peaks and temperature of maximum desorption, T_m

Sample	Area of the main peak at low temperature region $\times 10^8$	T_m (K)
K	0.07	437
K-ox1	0.61	421
K-ox3	2.58	412
K-Ni5	1.17	421
K-Co5	0.45	427
K-Mn5	0.34	421
K-ox1- Ni5	1.07	426
K-ox3- Ni5	2.83	419
K-ox3- Co5	1.59	409
K-ox3- Mn5	2.09	419

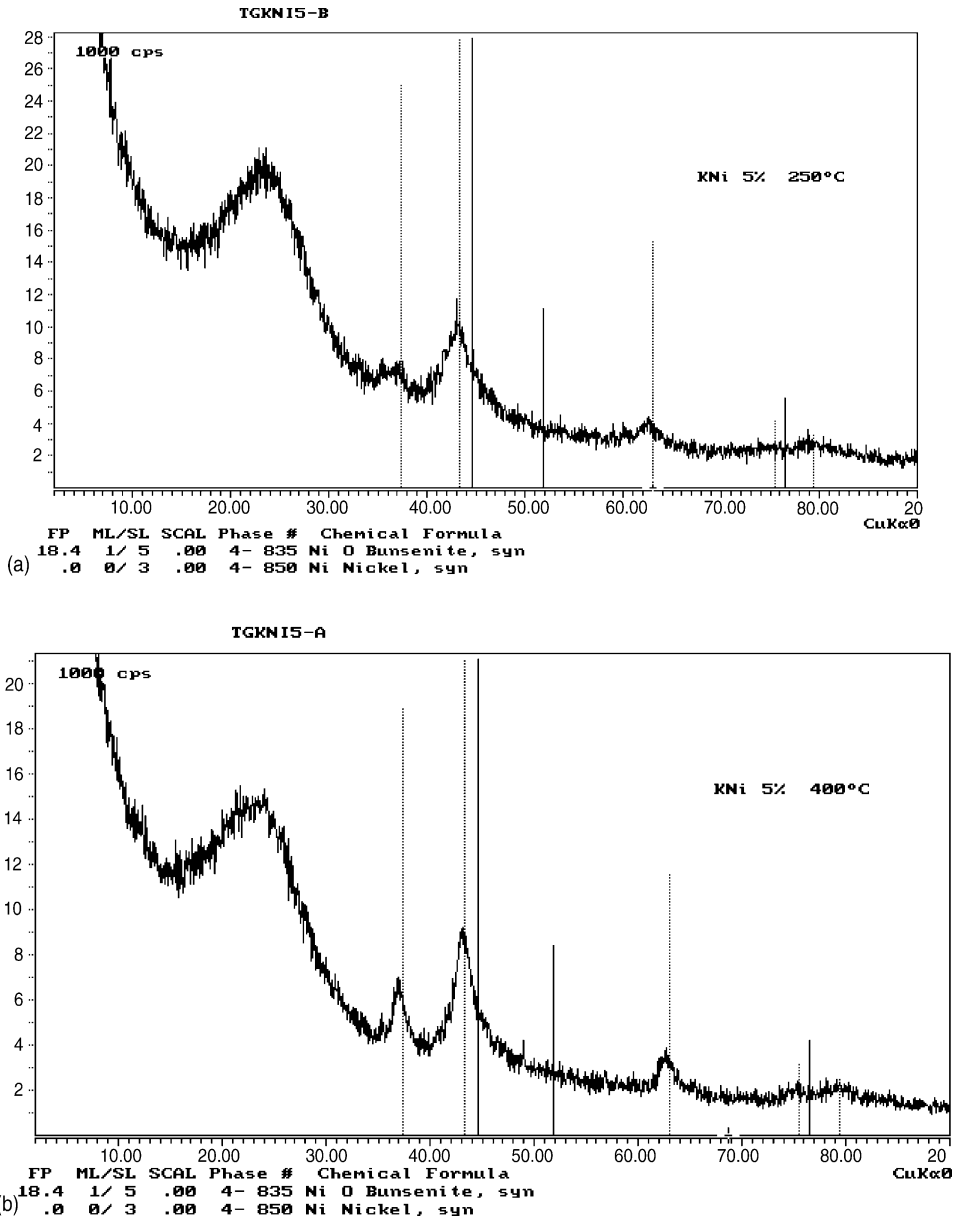

Fig. 3. (a, b) XRD patterns for K-Ni5 after calcinations at 523 and 673 K. (c, d) XRD patterns for K-Co5 after calcinations at 523 and 673 K.

3.1.2.2. X-ray diffraction. Fig. 3a–d shows XRD patterns for K-Ni5 and K-Co5 calcined at 523 and 673 K. The solid line indicates the angle position (2θ) of an appropriate metal (Co or Ni), while the dashed line coincides with nickel or cobalt oxides. From Fig. 3, it may be seen that for both samples K-Co5 and K-Ni5 after calcination at both temperatures, no reflexes for metallic Co or Ni were detected and active materials are present as oxides; Co_3O_4 and NiO (bunsenite), respectively. The peaks corresponding to graphitic structures are very broad indicating low graphitization degree for the used carbon fiber. The only difference between XRD patterns for calcination temperatures of 523 and 673 K is that the peaks for the samples calcined at 673 K were narrower testifying a more ordered structure (i.e. somewhat bigger crystallites). However, "big" crystallites were also identified by XPS for non-calcined sample (see further in the text). This would prove that there is not a basic change in dispersion after calcination. These experimental findings are in agreement with several indications in literature for Co- or Ni-promoted carbonaceous materials, as well as reactivity of carbon with oxides. Sharma et al. [35] showed that reaction between graphite and NiO took place very slowly below 1173 K. Zhu et al. [19] found no metallic Ni for Ni-promoted active carbons after calcination at 573 K although they found it after calcination at 773 K. Reduction of CoO supported on active carbon was found to start at calcination temperatures higher than 673 K [36]. Also cellulose-based active carbon impregnated with cobalt nitrate and calcined in argon at 673 K, showed only CoO and Co_3O_4 by XPS while XRD showed that the system was amorphous (no metallic Co was found either) [37]. Alvim-Ferraz et al. [38]

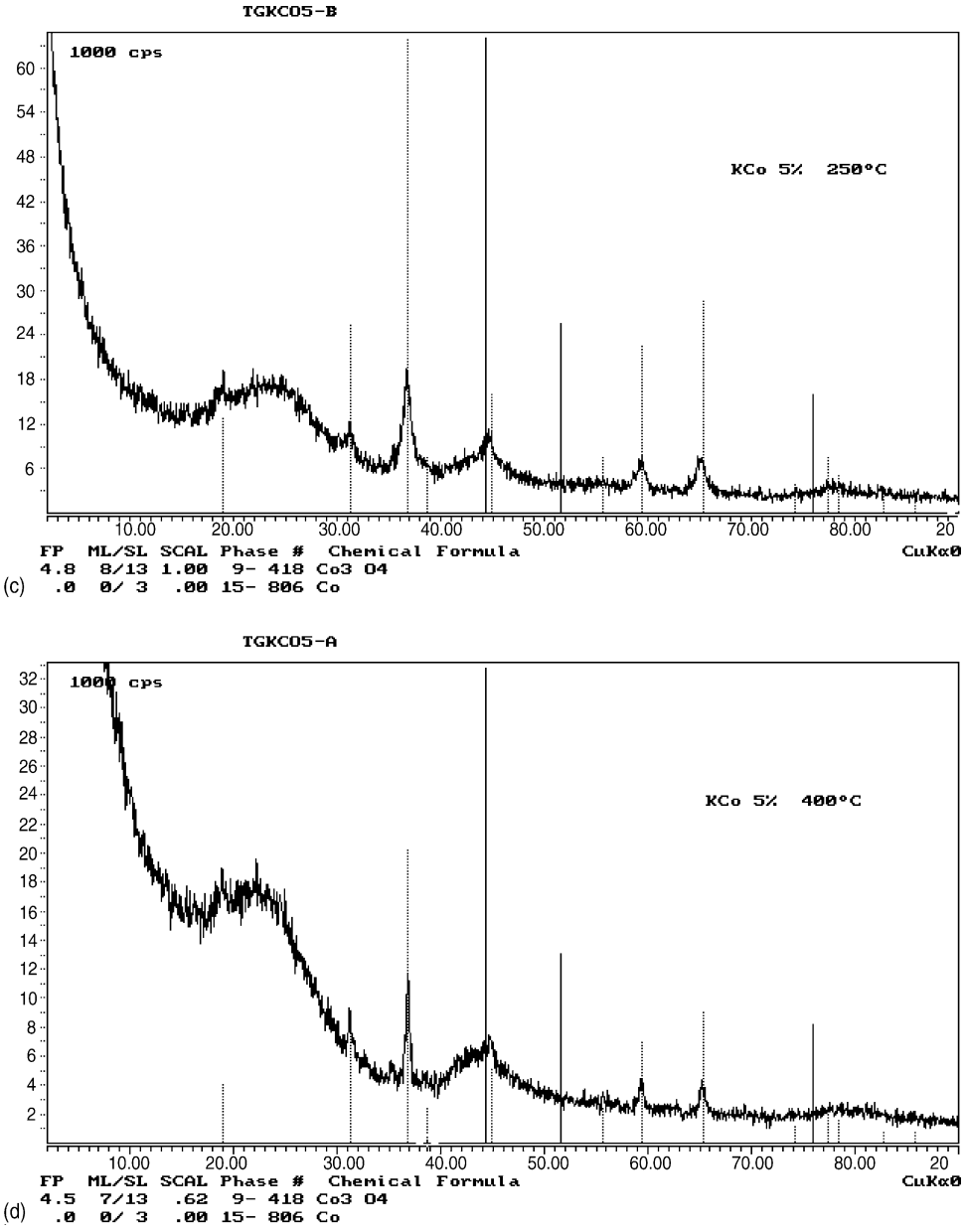

Fig. 3. (*Continued*).

used a somewhat different preparation procedure to obtain Co-promoted active carbon – precipitation of cobalt nitrate with sodium carbonate – and after calcination at 528 K only cobalt oxides (CoO and Co_3O_4) were found to be present in this case, as well.

3.1.2.3. Temperature-programmed desorption of ammonia (TPAD). Table 5 compares ammonia desorption for carbon fibers modified with Ni, Co or Mn oxides/hydroxides—the area of the low temperature peaks and temperature of maximum desorption.

From Table 5, the following conclusions may be drawn:

i. the addition of active material to carbon fiber K (unoxidized) increased the amount of adsorption sites for NH_3 to a different extent, depending on the type of active material. The amount of acid sites for Me–CF (Me = Ni, Co or Mn, carbon fiber (CF)) forms a sequence: K-Ni5 > K-Co5 > K-Mn5 ≫ K;
ii. the position and shape of the peaks were similar in all cases, suggesting weak acidic sites;
iii. the number of ammonia sorption sites for Ni-promoted differently pretreated carbon fibers forms a sequence: K-ox3-Ni5 > K-ox1-Ni5 ≈ K-Ni5. The number of sites on oxidized versus unoxidized support promoted with Co or Mn shows a similar tendency: K-ox3-Co5 > K-Co5 and K-ox3-Mn5 > K-Mn5;
iv. the comparison of K-ox3 and Ni, Co or Mn oxides/hydroxides-promoted catalysts shows that the number of sites increased only slightly for K-ox3-Ni5 and decreased

for K-ox3-Co5 and K-ox3-Mn5. This suggests that acidic sites are anchoring places for active material and their presence (or absence) will influence distribution, in good agreement with literature [18].

3.1.2.4. X-ray photoelectron spectroscopy (XPS). A typical XPS spectrum is shown for K-Ni5 in Fig. 4.

Binding energies registered for Me 2p peaks for the studied catalysts were:

- Ni-promoted: 855.7, 855.6 and 857.5 eV for K-Ni5, K-ox1-Ni5 and K-ox3-Ni5, respectively, corresponding to literature values for NiO (854.0–854.9 eV) or $Ni(OH)_2$ (855.98–856.4 eV) [39]. The peak observed at 857.5 may be connected with some remaining nitrate;
- Mn-promoted: at ca. 642.4 eV for K-Mn5 and 642.0 eV for both K-ox1-Mn5 and K-ox3-Mn5, indicating the presence of MnO_2/Mn_3O_4 [40–43];
- Co-promoted: at 784.4, 781.4 and 782.2 eV for K-Co5, K-ox1-Co5, K-ox3-Co5, respectively. All registered binding energies exceed literature values for CoO, CoOOH or $Co(OH)_2$, which are 779.5–780.5, 779.5 and 780.5 eV, respectively [44]. Thus, most probably there is a differential charging for K-Co5 and K-ox1-Co5, which may be expected for heterogeneous distribution with bigger crystallites on the surface, which as will be described later is the case for these samples. In case of K-ox3-Co5 with a much more even distribution of active material (see later in the text), it may be assumed that the unusually high binding energy is connected with the so-called binding energies shift. Such positive shifts have been observed for small clusters and isolated atoms on the supports [45,46];
- the main change registered for the calcined sample (K-Ni5c) was that instead of one peak for active material, two were found at 653.8 and 855.5 eV, which correspond

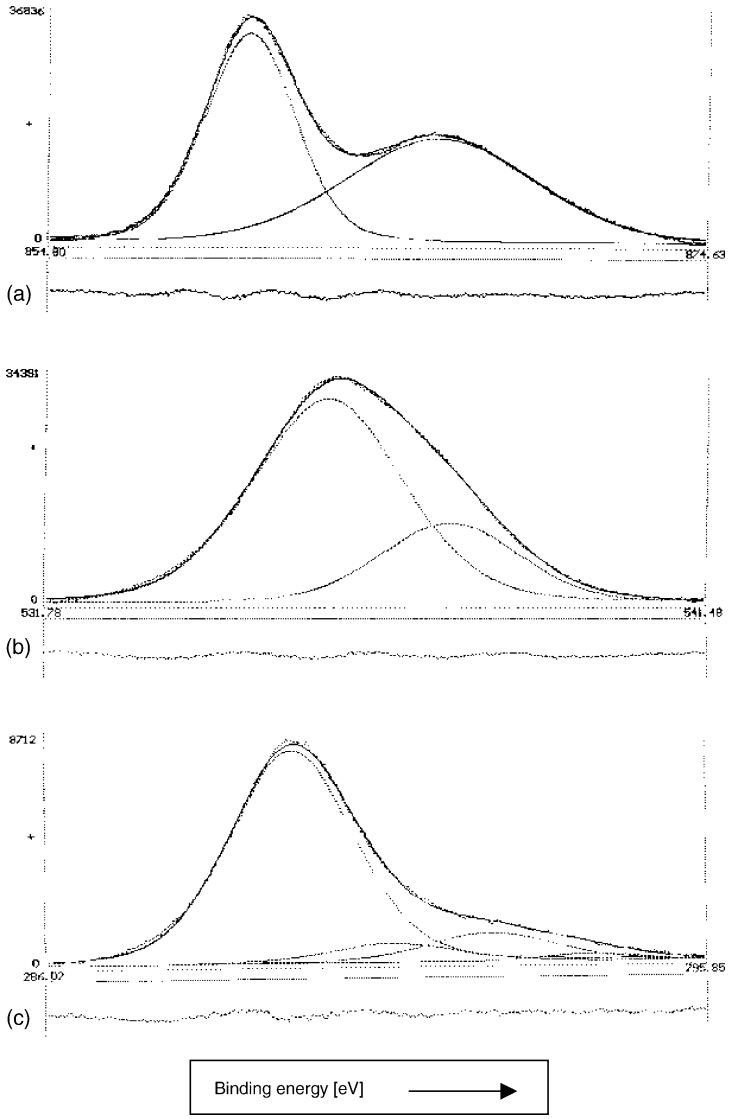

Fig. 4. XPS spectra for K-Ni5 (a) Ni $2p_{3/2}$, (b) O 1s, (c) C 1s.

Table 6
Surface composition of the studied samples (Me + C + O + N = 100%) and Me/C or O/C ratios (at.%/at. %)

Sample	Support	Amount of active material (wt.%/Me)	Surface composition (at.%)					
			Me	C	N	O	Me/C (at.%/at.%)	O/C (at.%/at.%)
K-Ni5	K	5 Ni	22.15	27.48	[a]	50.36	0.806	1.833
K-Ni5[b]	K	5 Ni	25.42	40.56	[a]	34.02	0.553	0.839
K-Ni5[c]	K	5 Ni	25.15	47.98	[a]	26.86	0.524	0.560
K-Co5	K	5 Co	11.96	49.13	[a]	38.91	0.243	0.792
K-Mn5	K	5 Mn	5.04	80.39	0.54	14.01	0.063	0.174
K-ox1-Ni5	K-ox1	5 Ni	11.11	56.23	[a]	32.67	0.198	0.581
K-ox3-Ni5	K-ox3	5 Ni	1.41	74.94	1.07	22.57	0.019	0.301
K-ox1-Co5	K-ox1	5 Co	2.83	79.30	[a]	17.88	0.036	0.225
K-ox3-Co5	K-ox3	5 Co	0.67	78.11	0.55	20.67	0.009	0.265
K-ox1-Mn5	K-ox1	5 Mn	1.84	82.32	[a]	15.84	0.022	0.192
K-ox3-Mn5	K-ox3	5 Mn	1.24	76.42	[a]	22.34	0.016	0.292

[a] Under detection level.
[b] Calcined at 523 K.
[c] After reaction of N_2O reduction.

to NiO (reference BE 854.4 eV) and $Ni(OH)_2$ (reference BE 855.9 eV), respectively. No peak connected with metallic nickel (reference BE 852.7 eV) [47] was found. This is in good agreement with XRD data discussed above;

- catalyst after reaction of N_2O decomposition in the absence of oxygen in reaction mixture at the whole temperature sequence up to 693 K (designated K-Ni5r) again showed two Ni $2p_{3/2}$ XPS peaks at 854.1 and 856.0 eV, corresponding to NiO and $Ni(OH)_2$.

Table 6 summarizes the surface composition for the studied catalysts. From Table 6, it may be seen that the amount of surface Ni (or Co, or Mn) depends on the pretreatment of the support. This is additionally illustrated in Fig. 5a and b, showing that XPS atomic ratios of Ni/C, Co/C and Mn/C [at.%/at.%] differ considerably, depending on the pretreatment of the support.

The dispersion of active material cannot be seen in a straightforward way from XPS intensity values, as intensity ratio depends on the texture of the catalysts and varies with the changes in specific surface area. Thus, in order to prove that dispersion is totally different for K- and K-ox3-supported catalysts, calculations based on the model of Kerkhof and Moulijn were carried out using an equation [48]:

$$\left(\frac{I_p}{I_s}\right) = \left(\frac{p}{s}\right)_b (1-x)\frac{E_s}{E_p}\frac{\sigma_p}{\sigma_s}\frac{\beta_1}{2}\frac{(1-e^{-\beta_2})}{(1+e^{-\beta_2})}$$

with p and s are promoter and support; I XPS intensity; x the promoter fraction (weight) in the final catalyst, σ the XPS cross-section, $\beta_1 = t/\lambda_{ss}$, $\beta_2 = t/\lambda_{pp}$, λ the escape depth of the appropriate electrons.

For calculations, the following parameters were taken: C content 92.7 and 93.6 wt.% for K and K-ox3, as determined by elemental analysis, specific surface areas of catalysts as presented in Table 2, density 1.8 g/cm^3, σ for C 1s, Ni $2p_{3/2}$, Co $2p_{3/2}$ and Mn 2p; 1.0, 13.92, 12.20 and 13.62, respectively, from the article of Scofield [49], and λ calculated from equation of Chang [50].

Experimentally measured intensity ratios $(I_p/I_s)_{exp}$ were found in literature to be:

- equal to those calculated from the model $(I_p/I_s)_{calc}$, testifying to a monolayer distribution of active material;
- higher or much higher than the calculated ones when there was a preferential deposition of active material (in the

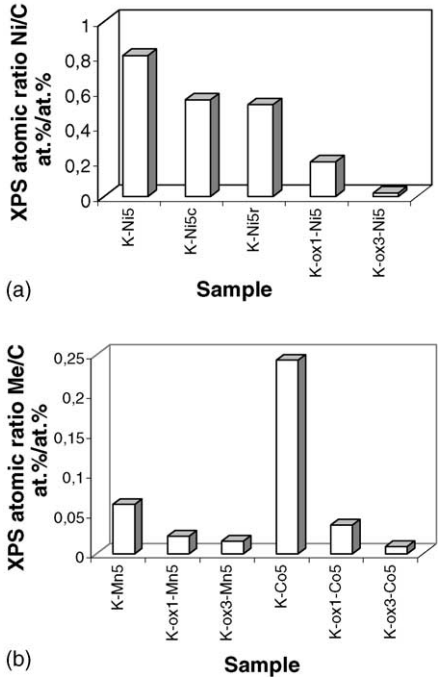

Fig. 5. (a) Surface Ni/C ratios (at.%/at.%) for Ni-promoted carbon fibers untreated or differently pretreated (c-calcined, r-after reaction of N_2O reduction). (b) Surface Me (Mn or Co)/C ratios (at.%/at.%) for Mn- or Co-promoted carbon fibers untreated or oxidized at 343 K or boiling temperature.

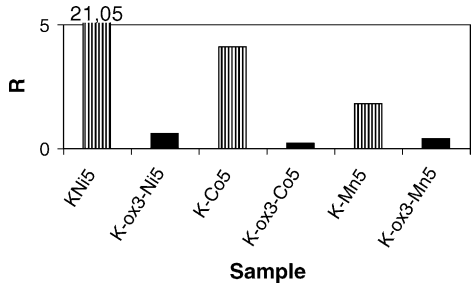

Fig. 6. $R = (I_p/I_s)_{exp}/(I_p/I_s)_{calc}$ for catalysts supported on K or K-ox3: $(I_p/I_s)_{exp}$ is intensity ratio of promoter p (Ni $2p_{3/2}$, Co $2p_{3/2}$, Mn 2p) to supports (C 1s) measured experimentally; $(I_p/I_s)_{calc}$ the intensity ratio of promoter to support calculated from the model of Kerkhof and Moulijn.

form of bigger crystallites) on the outer surface of the grains of the support; or
- smaller than $(I_p/I_s)_{calc}$, if outer surface was depleted in active material, which formed discrete crystallites on the inner surface of the support.

Fig. 6 shows parameter R defined here as the ratio of I_p/I_s measured experimentally to I_p/I_s calculated from the model ($R = (I_p/I_s)_{exp}/(I_p/I_s)_{calc}$). The picture illustrates the following: (i) the mentioned ratio is higher or much higher than 1 for K-based catalysts. This means that there is a preferential enrichment at the outer surface (and thus bigger crystallites are present); (ii) the ratio is approaching 1 (it is ca. 0.7, but it must be taken into account that the model is rather rough) for K-ox3-Ni5 and definitely smaller than 1 for K-ox3-Mn5 and K-ox3-Co5 (ca. 0.4 and 0.2, respectively), indicating the enrichment of the inner surface and the formation of smaller crystallites and/or clusters of MeO_x. The argument is of course not only based on the model of Kerkhof and Moulijn in this case, because the model itself only points to crystallites on the inner surface. However, taking into account that the supports are exclusively microporous, the formation of bigger crystallites e.g. 3 nm in size inside micropores is not possible because they would totally block the porous system, which does not contain any mesopores. Smaller units and partial blocking are possible as the specific surface area decreased for catalysts in comparison to the support.

A similar tendency to that presented in Fig. 6 was observed for numerous transition metal oxide-promoted active carbons, e.g. Mn/active carbon [20] or Ni/active carbon [18] although in the latter case, the difference between catalysts on unoxized and oxidized support was ca. 4.0 and thus there was a much more even distribution than in the case reported here. A possible explanation may be much easier accessibility of micropores in carbon fibers in comparison to active carbons.

3.1.2.5. Temperature-programmed reduction. Fig. 7a–d shows temperature-programmed reduction of supports and Ni-, Co- or Mn-promoted carbon fibers untreated or oxidatively pretreated. It must be taken into account that apart from the reduction by hydrogen, additional reduction effects may be expected due to the presence of carbonaceous support. From Fig. 7, it may be seen that:

(i) the reduction of K and K-ox3 produced only a high temperature peak, indicating a small amount of oxygen on the surface of K and a three times higher amount for K-ox3;
(ii) the introduction of active material resulted in the increase of oxygen amount on the surface to an extent depending on the type of active material and the pretreament of the support;
(iii) catalysts on oxidatively pretreated support K-ox3 have a different distribution of sites from those of K-based catalysts, either the maximum shifts to higher temperature (K-Co5 versus K-ox3-Co5) or the peak is broadened (K-Ni5 versus K-ox3-Ni5, K-Mn5 versus K-ox3-Mn5), suggesting additional less labile oxygen present.

3.2. Reduction of N_2O with carbon

Typical experimental results for N_2O reduction with carbon are shown in Fig. 8 for K-Ni5. Fig. 8 shows the amount of N_2O and CO_2 in the products as a function of temperature. From the figure, it may be derived that the reaction started at ca. 573 K. The amount of dinitrogen oxide decreased while the amount of produced CO_2 increased. The amount of CO_2 was almost identical with the amount of reduced N_2O, which suggests a stoichiometry of 1:1. As the reaction $2N_2O + C \rightarrow CO_2 + 2N_2$ suggests a stoichiometry of two molecules of N_2 to one molecule of CO_2, this means that more CO_2 is produced than forecast by the above reaction. This may imply either a secondary reaction (e.g. desorption of oxygen-containing groups from the surface in the form of CO_2) or a reaction of N_2O with C(O) sites rather than with C-sites.

Fig. 9 compares all catalysts for the studied temperatures of 453–693 K in the form of the amount of reduced N_2O and formed CO_2 (in ppm). From the figure, it may be seen that the produced amounts of CO_2 in all cases drastically exceed those predicted by reaction of N_2O with C-sites. Let us assume that some CO_2 originates from oxygen-containing surface species on the surface having nothing to do with nitrous oxide; they can desorb from the surface and therefore may appear in the products before any N_2O was reduced. Fig. 9 shows that this is the case for K-Co5, K-ox3-Co5, K-Mn5, K-ox3-Mn5 and K-ox3-Ni5. Thus, some carbon dioxide definitely did not originate from N_2O reduction. No such effect is present for K-Ni5. Therefore, it may be speculated that at least some of carbon dioxide originated from the secondary reaction. It is not possible under the conditions of this experiment to differentiate between CO_2 originating from surface groups decomposition and those formed with oxygen originating from N_2O. It would be possible only in an experiment with labeled oxygen.

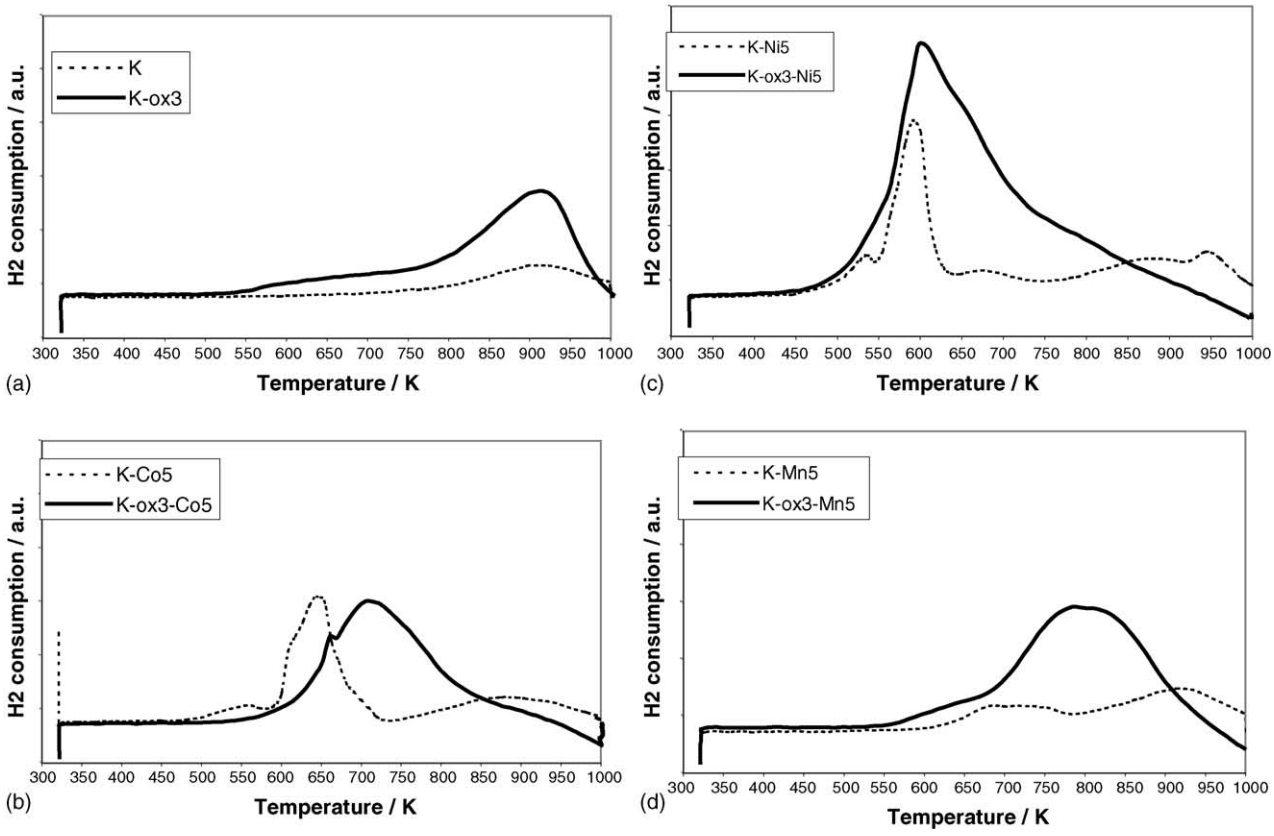

Fig. 7. (a–d) Temperature-programmed reduction of the supports and studied catalysts.

However, the explanation that CO_2 comes to the same extent from the surface for K- and K-ox3-based catalysts is in itself unreasonable, because there is a different amount of surface oxygen bound in acidic groups (and those give CO_2 as a decomposition product) for K and K-ox3. Therefore, if the effect originated only in some desorption effects irrespective of the reaction, the unbalance should be much smaller for K-based than K-ox3-based samples, and from Fig. 9, it may be seen it is not so. Therefore, the additional amounts of CO_2 must originate from the reduction reaction. In order to take into account, at least roughly the ''direct desorption'' products, the amount desorbed at the highest temperature, where still no reaction with nitrous oxide took place was subtracted from the total amount of CO_2 and added as a third curve in Fig. 9. These curves show that the unbalance is still there to a higher extent for K-ox3-based samples than for K-based ones. This would be an argument for rather than against the participation of C–O complexes because K-ox3 surface is, on the whole, more oxidized than that of K. Thus, it may be suggested that at least some of carbon dioxide comes from the proposed interaction of oxygen from N_2O with C–O species on the surface. It may not be the only mechanism but it seems reasonable that it may be one of them. This finds some indirect substantiation in the work of Yang et al. [51] if NO reduction may be assumed to have a similar mechanism as N_2O, which is generally believed in literature. Yang et al. [51] showed on carbon black that more thermally stable C–O complexes play an important role in the enhancement of reaction rate by activating the neighbouring carbon atoms. Thus, stoichiometries of N_2 to CO_2 of 1:over 0.5 (as e.g. for Dandekar and Vannice[24]) would support the presented hypothesis. As, however, some catalysts e.g. Cu/active carbon of Zhu et al. [18] did not show this effect, the relative importance of the proposed route is still open to discussion.

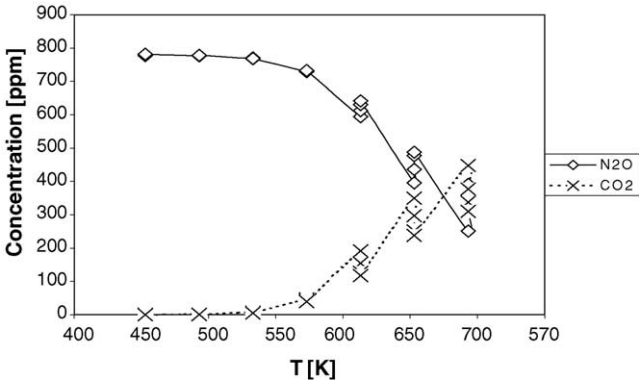

Fig. 8. N_2O and CO_2 on stream in N_2O reduction with carbon K-Ni5.

Fig. 10 shows the comparison of N_2O conversion for carbon fibers modified with different transition metal oxides/hydroxides. The introduction of oxides of Ni, Co or Mn increased N_2O conversion and forms a sequence:

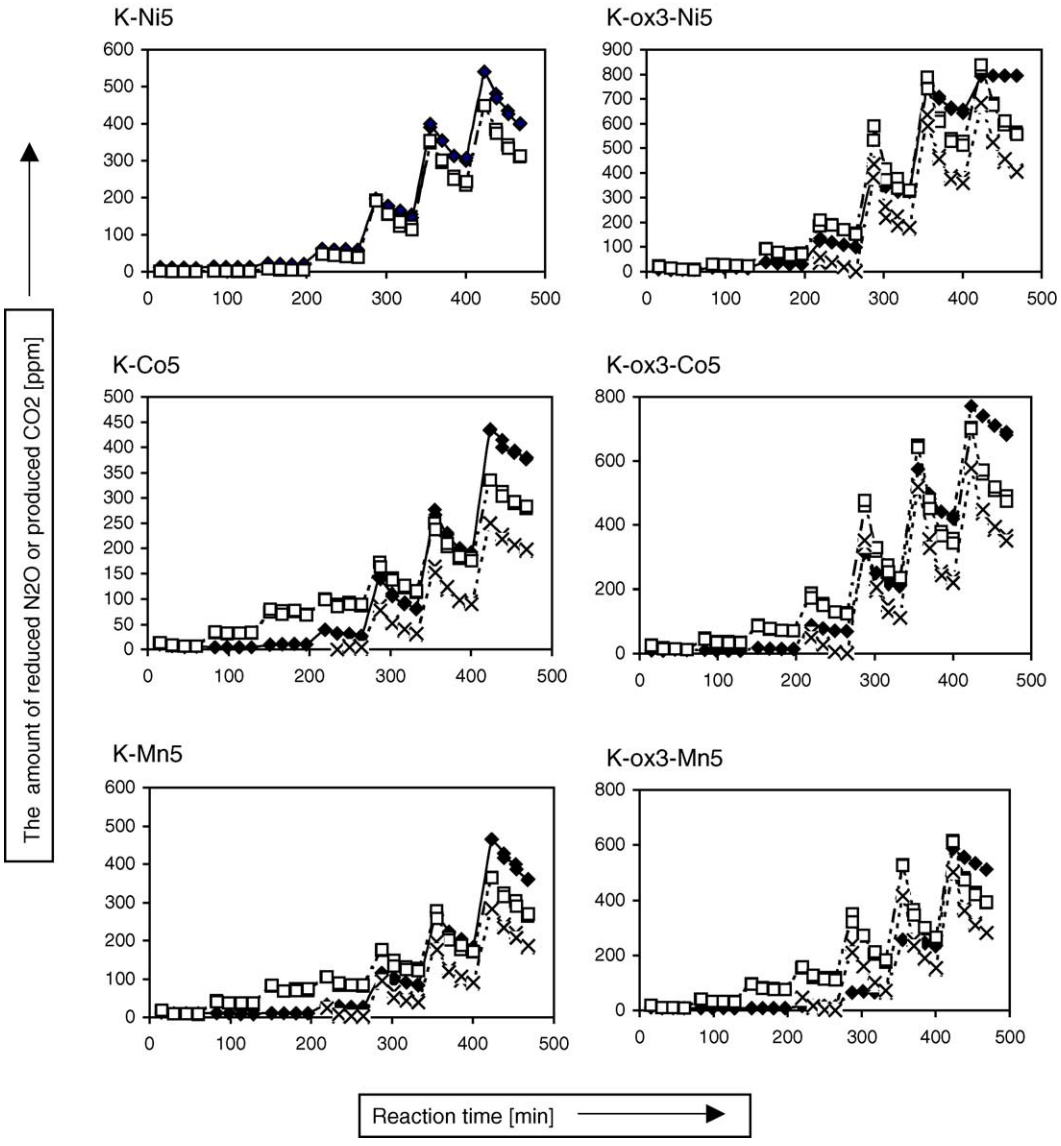

Fig. 9. N_2O and CO_2 on stream in N_2O reduction with carbon at 453, 493, 533, 573, 613, 653 and 693 K for 60 min at each temperature. (◆) Amount of removed N_2O (initial N_2O concentration – N_2O concentration in the products); (□) amount of produced CO_2; (×) CO_2^* (total CO_2 amount in the products – amount of CO_2 at the highest temperature without N_2O reduction (see text)). (For K-Ni5, CO_2 did not appear in the products before N_2O reduction started and thus CO_2^* curve and CO_2 are overlapping.)

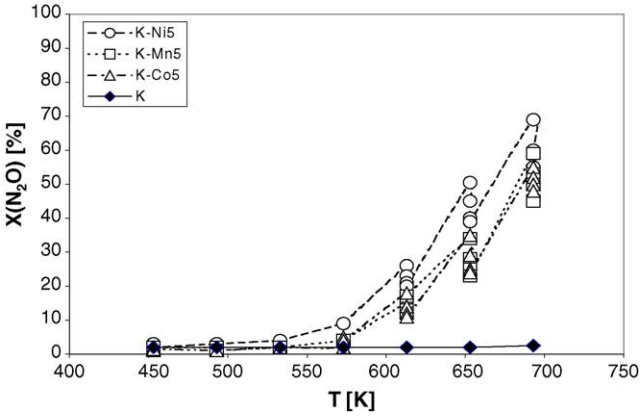

Fig. 10. N_2O conversion for carbon fiber K modified with Ni, Co or Mn oxides/hydroxides.

K-Ni5 > K-Mn5 ≈ K-Co ≫ K. N_2O conversion increased with temperature. At 693 K, it was between ca. 55 and 70%.

Fig. 11 shows the comparison of N_2O conversion for catalysts supported on oxidized carbon fiber K-ox3. The conversions form a sequence: K-ox3-Ni5 > K-ox3-Co5 > K-ox3-Mn5 ≫ K-ox3. Conversions were much higher for samples based on pretreated (initially oxidized) supports. The direct comparison with the results of Zhu et al. [18] for Ni-promoted active carbons is not possible as the reaction of Zhu was carried out isothermally at 573 or 673 K, while our catalysts underwent sequential increase of temperature and thus the first measured point on higher temperature corresponds to a catalyst already partly deactivated at lower temperature. The general picture is, however, similar, at 573 K the difference between K-Ni5 and K-ox3-Ni5 is below 10% and at 693 K, ca. 50% of N_2O conversion.

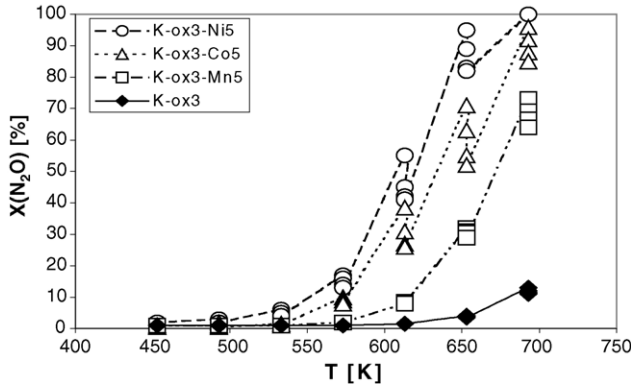

Fig. 11. N_2O conversion for oxidized carbon fiber (K-ox3) promoted with Ni, Co or Mn.

The fact that the oxidized support reduced ca. 10% N_2O, while untreated support K was inactive stresses the role of oxygen-containing groups present on the surface. Either oxygen transfer is thus facilitated or as suggested by Yang et al. [51] for NO reduction by carbon, C–O complexes activate the neighbouring carbon atoms leading to the enhancement of reaction rate.

Both Figs. 10 and 11 show that the studied samples deactivate on stream, the rate of deactivation increasing with temperature. This is expressed by four points measured at each temperature (every 15 min). Similar observations may be made from Fig. 9, where the amount of removed N_2O (in ppm) is shown as a function of time for all studied temperatures 453–693 K. For higher temperatures 613, 653 and 693 K, it may be observed that each of these temperatures starts with higher conversion and is followed by three measurements, taken after 30, 45 and 60 min on line, showing (each of them) lower amount of N_2O removed from stream in comparison to the previous experimental point. The extent of deactivation is different for K- and K-ox3-based catalysts and depends additionally on active material. There is only one point for K-ox3-Ni5 in Fig. 11 which, however, does not mean the lack of deactivation but rather the fact that the sample was so active that even the decrease in N_2O did not register as decreased conversion.

The difference in N_2O conversion for the same type of active material ($NiO/Ni(OH)_2$ or $CoO/Co(OH)_2$ or MnO_x) but different supports (cf. Figs. 10 and 11) shows that the acidic pretreatment of carbon fibers had a considerable influence on the N_2O reduction activity. Similar observations were made by Zhu et al. for active carbons promoted with Ni [18] or Cu [19]. This observation should be related to the influence of acidic pretreatment on the distribution of active material. As discussed in 2.4, acidic pretreatment totally changed the distribution of active material. This implies a more facile dissociative chemisorption on smaller units of active material (small crystallites clusters and/or individual cations) than on bigger microcrystallites. This effect was not so evident for Cu/AC or Cu/AC–HNO_3 or Ni/AC and Ni/AC–HNO_3 samples of Zhu et al. [18,19] which showed similar N_2O reduction but it must be also stressed that differences in distribution of Ni are much bigger in our case.

On the other hand, deactivation was greater for oxidatively pretreated catalysts, which was also found for Ni on active carbon [18] and to a smaller extent, for Cu on active carbon [19].

The mechanism discussed by Zhu et al. [19] suggests that the main cause of deactivation lies in the fact that the transfer of oxygen from Ni to carbon is more difficult on untreated in comparison to pretreated active carbons. However, the effect seems to be totally different for our catalysts. The number of decomposed N_2O molecules was linearly related to the number of produced CO_2 during deactivation at each temperature (613, 653, 693 K) for K-Mn5, K-Ni5 and K-Co5 while the amount of CO_2 decreased more steeply for K-ox3-based catalysts (K-ox3-Co5 and K-ox3-Mn5). A similar observation was made for K-ox3-Ni5 at 613 and 653 K. At 693 K, conversion of N_2O was very high for K-Ni5 and no deactivation effect was observed for N_2O as mentioned before. Thus, oxygen transfer seems more facile for K-Me samples than K-ox3-Me samples. The explanation for this behaviour may be connected with the lability of oxygen on the catalysts (cf. Fig. 7). For the former, TPR peaks were observed at lower temperatures while for the latter, the distribution of oxygen sites was much broader and/or with a maximum at higher temperatures. This suggests that lattice oxygen on K-based samples is more labile and easier to remove, and thus possibly easier to transfer to the support to form CO_2. Curtin et al. [22] found such a correlation between TPR profiles and N_2O formation for CuO/Al_2O_3 catalyst for NH_3 oxidation. The explanation given was that labile surface oxygen increased the average oxidation state of the monoatomic nitrogen pool which led to N_2O formation. Reducing the oxygen mobility decreased this effect.

Fig. 12 gives a comparison of N_2O conversion for K-Ni5 and K-ox3-Ni5 in the presence and absence of oxygen. As it may be seen from the picture, conversions are much lower in

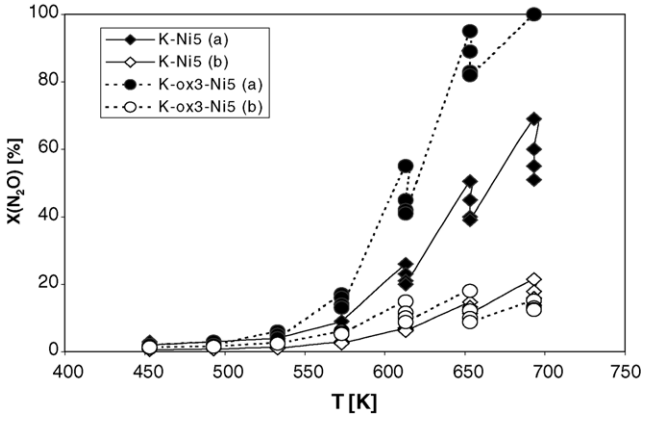

Fig. 12. N_2O conversion for Ni-promoted carbon fibers (a) in the absence of oxygen and (b) in the presence of oxygen.

the presence of oxygen but are still discernible at higher temperatures. Thus, a secondary mechanism of N_2O reduction is possible. Nevertheless, the process in the presence of oxygen is accompanied by high CO_2 production, especially in the case of K-ox3-Ni5, rendering this sort of catalyst rather impractical for N_2O decomposition as such.

There is an additional question to what extent the findings of this work may be generalized for all carbonaceous materials, taking into account differences between active carbons, which were most often studied in that respect, and carbon fibers. There are in principle two main differences in structure between carbon fibers and active carbons. The first is connected with differences in the porosity; both system are mainly microporous but the accessibility of micropores is different in both cases: they are directly accessible from the outer surface for carbon fibers and through a complicated system of macro and mesopores for active carbons. Thus, the kinetics may be influenced [52]. However, as no kinetics are considered here this does not seem to be the point. The second difference is the presence of ash in active carbons (no ash in carbon fibers). This seems more to the point, because some of ash components may be catalytically active. There were e.g. considerable amounts of ash in active carbons (5.6–7.4 wt.%) studied by Zhu et al. [19] and taking this into account it may be assumed that no additional catalytic effects may be expected in our carbon fibers in comparison to those of Zhu, where they cannot be absolutely excluded. Thus, carbon fibers may be treated as model systems in that respect. Where oxidative pretreatment of the surface is concerned, quantitative but not qualitative differences may be expected. Several articles in literature showed that oxidative pretreatment had similar effect on active material distribution for active carbon- and carbon fiber-based catalysts. As examples, articles of Grzybek et al. [10] and Marban et al. [11–13] may be quoted. In the former case, Mn was introduced onto active carbons and in the latter, on carbon fibers in both cases untreated or oxidized. Generally, the influence of surface groups on distribution was quite similar.

4. Conclusions

Carbon fiber-supported nickel, cobalt or manganese oxides may reduce N_2O. The overall effect depended on the initial pretreatment of the support. The origin of the effect lies in different distribution of active material, which was influenced by the type, as well as number of surface oxygen functionalities. Only oxidative pretreatment carried out under desired conditions (e.g. at high temperature) produced appropriate type/number of groups resulting in small crystallites clusters and/or individual atoms of active material distributed on the inner surface of the support. The absence of acidic surface groups or their low number may lead to the deposition of bigger crystallites of active material predominantly on the outer surface of a support. The existence of varying types of distribution of active material resulted also in different reducing conditions and thus influenced the lability of surface oxygen. This, in turn, affected oxygen transfer from active material to the support. The presence of more labile oxygen resulted in easier transfer and faster formation of CO_2 and thus slower deactivation. On the other hand, distribution may be also responsible for different behaviour concerning dissociative chemisorption of N_2O.

Acknowledgments

The support of this work by DAAD-KBN exchange programme has been greatly appreciated (Polish project no. AGH no.11.11.210.62, German project no. D/02/32230 in the programme PPP Polen).

The authors would like to thank Kynol Europa GmbH for supply of Kynol sample.

References

[1] T. Grzybek, M. Rogóż, H. Papp, Catal. Today 90 (2004) 61.
[2] H. Yamashita, H. Yamada, A. Tomita, Appl. Catal. 78 (1991) L1.
[3] M.J. Illan-Gomez, E. Raymundo-Pinero, A. Garcia-Garcia, A. Linares-Solano, C. Salinas-Martinez de Lecea, Appl. Catal. 20 (1999) 267.
[4] M.J. Illan-Gomez, A. Linares-Solano, C. Salinas-Martinez de Lecea, Energy Fuels 9 (1995) 976.
[5] D. Mehandjiev, M. Kristova, E. Bekyarova, Carbon 34 (1996) 757.
[6] M. Kristova, D. Mehandjiev, Carbon 36 (1998) 1379.
[7] M.J. Illan-Gomez, A. Linares-Solano, C. Salinas-Martinez de Lecea, Energy Fuels 9 (1995) 112.
[8] H. Yamashita, A. Tomita, Energy Fuels 7 (1993) 85.
[9] J. Pasel, P. Käßner, B. Montanari, R. Dziembaj, H. Papp, Appl. Catal. B 18 (1998) 1999.
[10] T. Grzybek, M. Rogóż, J. Pasel, H. Papp, Phys. Chem. Chem. Phys. 1 (1999) 341.
[11] G. Marban, A.B. Fuertes, Appl. Catal. B 34 (2001) 43.
[12] G. Marban, Appl. Catal. B 41 (2003) 323.
[13] G. Marban, A.B. Fuertes, Appl. Catal. B 34 (2001) 55.
[14] T. Grzybek, H. Papp, Appl. Catal. B 1 (1992) 271.
[15] M. Yoshikawa, A. Yasutake, I. Mochida, Appl. Catal. A 173 (1998) 239.
[16] M.J. Lazaro, M.E. Galvez, I. Suelves, R. Moliner, S.V. Vassilev, C. Braekmen-Danheux, Fuel 83 (2004) 875.
[17] Z. Zhu, Z. Liu, S. Liu, H. Niu, Appl. Catal. B 23 (1999) 229.
[18] Z.H. Zhu, L.R. Radovic, G.Q. Lu, Carbon 38 (2000) 451.
[19] Z.H. Zhu, S. Wang, G.Q. Lu, D.-K. Zhang, Catal. Today 53 (1999) 669.
[20] T. Grzybek, J. Klinik, M. Rogóż, J. Pasel, H. Papp, J. Chem. Soc., Faraday Trans. 94 (1998) 2843.
[21] T. Grzybek, J. Klinik, P. Czajka, P. Niemczyk, H. Papp, Polish J. Environ. Studies, 2005, in press.
[22] T. Curtin, F.O. Regan, C. Deconinck, N. Knüttle, B.K. Hodnett, Catal. Today 55 (2000) 189.
[23] T. Grzybek, J. Klinik, A. Krzyżanowski, H. Papp, Pol. J. Environ. Sci. 11 (2002) 49.
[24] A. Dandekar, M.A. Vannice, Appl. Catal. B 22 (1999) 179.
[25] L.A. Boot, M.H.J.V. Kerkhoffs, A.J. Van Dillen, J.W. Geus, F.R. Van Buren, B.Th. Van der Linden, Appl. Catal. A 137 (1996) 69.

[26] C.D. Wagner, L.H. Gale, R.H. Raymond, Anal. Chem. 51 (1979) 466.
[27] J.L. Figueiredo, M.F.R. Pereira, M.M.A. Freitas, J.J.M. Orfao, Carbon 37 (1999) 1379.
[28] K. Jurewicz, K. Babeł, A. Ziółkowski, H. Wachowska, M. Kozłowski, Fuel Process. Technol. 77–78 (2002) 191.
[29] K. Jurewicz, K. Babeł, A. Ziółkowski, H. Wachowska, Electrochim. Acta 48 (2003) 1491.
[30] T.J. Bandosz, B. Buczek, T. Grzybek, J. Jagiełło, Fuel 76 (1997) 1409.
[31] C. Moreno-Castilla, F. Carrasco-Marin, F.J. Maldonado-Hodar, J. Rivera-Utrilla, Carbon 36 (1998) 145.
[32] G.S. Szymański, T. Grzybek, H. Papp, Catal. Today 90 (2004) 51.
[33] S. Biniak, G. Szymański, J. Siedlewski, A. Świątkowski, Carbon 35 (1997) 1799.
[34] S.S. Barton, M.J.B. Erans, E. Halliop, J.A.F. MacDonald, Carbon 35 (1997) 1799.
[35] S.K. Sharma, F.J. Vastola, P.L. Walker Jr., Carbon 34 (1996) 1407.
[36] D. Mehandjiev, E. Bekyarova, J. Colloid Interf. Sci. 166 (1994) 476.
[37] J.S. Moon, K.K. Park, J.H. Kim, Appl. Catal. A 201 (2000) 81.
[38] M.C.M. Alvim-Ferraz, C.M. Todo-Bom Gaspar, J. Coloid Interf. Sci. 259 (2003) 133.
[39] E. Paparazzo, Surf. Interf. Anal. 12 (1983) 115.
[40] M. Oku, K. Hirokawa, S. Ikeda, J. Electron. Spectrosc. 7 (1975) 465.
[41] M. Oku, K. Hirokawa, J. Electron. Spectrosc. 8 (1976) 475.
[42] V. Dicastro, C. Furlani, M. Gargano, M. Rossi, Appl. Surf. Sci. 28 (1987) 270.
[43] J.W. Murray, J.G. Dillard, R. Giovanoli, H.M. Moers, W. Stumm, Geochim. Cosmochim. Acta 49 (1985) 463.
[44] N.S. McIntyre, M.G. Cook, Anal. Chem. 47 (1975) 2208.
[45] S. Kohiki, Appl. Surf. Sci. 25 (1986) 81.
[46] A.R. Gonzales-Elipe, G. Munuera, J.P. Espinos, Surf. Interf. Anal. 16 (1990) 375.
[47] D. Briggs, (Ed.), Practical Surface Analysis, vol. 1, Auger and X-ray photoelectron, 1990.
[48] F.P.J.M. Kerkhof, J.A. Moulijn, J. Phys. Chem. 83 (1979) 1612.
[49] J.H. Scofield, J. Electron. Spectrosc. 8 (1976) 129.
[50] C.C. Chang, Surf. Sci. 48 (1975) 9.
[51] J. Yang, G. Mestl, D. Herein, R. Schögl, J. Find, Carbon 38 (2000) 729.
[52] I. Mochida, Y. Korai, M. Shirahama, S. Kawano, T. Hada, Y. Seo, Carbon 38 (2000) 227.